THERMOELASTIC STRUCTURES FOR HIGH DENSITY ULTRASONIC ENERGY

R.J. von Gutfeld and D.R. Vigliotti
IBM Thomas J. Watson Research Center
Yorktown Heights, NY 10598

C.S. Ih
University of Delaware
Newark, DE 19711

W.R. Scott
NADC
Warminster, PA 18974

The use of lasers to generate thermoelastic waves has received considerable attention since the publication of the theoretical work of White.[1] The author derives equations for the propagation of longitudinal elastic waves produced by surface heating of a semi-infinite medium with harmonic thermal (laser) excitation. The importance of the boundary conditions in determining the magnitude of the resulting elastic waves is described. Two conditions are imposed and the resulting amplitudes derived: (1) Laser absorption at x = 0 with elastic amplitude u=0 at x = 0 for all times $t \geq 0$ (perfectly clamped or constrained surface) and (2) for the stress $\sigma = 0$ at x = 0 for $t \geq 0$ (free surface). Propagation of the elastic wave is in the x direction. The one dimensional solutions for the strain amplitudes $\delta u/\delta x = \varepsilon$, under these two sets of boundary conditions are

$$\varepsilon = \frac{k\tau\alpha\Theta_o}{k^2+\tau^2} \text{ (constrained)} \tag{1}$$

and

$$\varepsilon = \frac{k^2\alpha\Theta_o}{k^2+\tau^2} \tag{2}$$

where α is the coefficient of thermal expansion, Θ_o the maximum harmonic temperature excursion at the surface, $k = 2\pi/\lambda$ with ω the harmonic angular frequency of the incident radiation, v the longitudinal elastic velocity of the propagating wave and $\tau = \sqrt{\omega/2\kappa}$, the thermal skin depth with κ the thermal diffusivity of the optically absorbing medium.

It was considerably later that von Gutfeld and Melcher showed that laser generated elastic waves could also be used for nondestructive testing.[2] The advantage of the laser as an elastic generator is (1) a steerable beam source, and (2) a variable source diameter determined by the laser spot size at the point of incidence on the sample or optical absorber. Initial experiments were carried out at 20 MHz using a partially clamped surface, constrained by means of an optically transparent dielectric plate. A PZT, 20 MHz receiver was used to detect the transmitted waves generated by means of a pulsed dye laser with $\sim$5 ns pulses. It was shown experimentally that the ratio of clamped to unclamped strain amplitude is on the order of 100 at 20 MHz as predicted by the ratio R of the two amplitudes (Eq. 1 to Eq. 2), i.e.,

$$R = \frac{v}{(\kappa\omega)^{1/2}} \quad . \tag{3}$$

Subsequently, an analysis of three layered elastic wave generating structures was undertaken using the basic derivations of Ref. 1 and matching thermal and elastic boundary conditions at each interface.[3] Pulses were treated as a superposition of sine waves. Investigations on a number of three layered thermoelastic generators were made to increase the conversion efficiency, η, of optical to elastic power densities. It was found that a judicious choice of materials can increase the efficiency by almost 2 orders of magnitude. Typically, a controlled heat leak into a liquid such as water, alcohol or acetone from a thin optically absorbing film was found to be relatively more efficient, but even for the best structures the conversion efficiency is still relatively small. Table 1 summarizes the maximum conversion efficiency possible per watt/cm^2 of absorbed optical flux, assuming perfect clamping at the absorbing surface by a perfect thermal insulator. Since no heat loss can occur to the clamping medium, this hypothetical structure will provide maximum elastic conversion into the medium of interest. The values of Table 1 are calculated from the theory of Ref. 1, where we use the relations,

$$\eta = I_{elastic}/I_{absorbed} \tag{4}$$

and

$$I_{elastic} = (\frac{v}{2})\sigma_{xx}\varepsilon^*_{xx} \quad . \tag{5}$$

With appropriate substitutions the efficiency, η, can be rewritten in the form

$$|\eta| = \frac{5.7\times10^{-9} v\alpha\, I_o}{\rho C^2} \tag{6}$$

where I_o is the absorbed incident flux (w/cm^2), C, the heat capacity (cal/gm^o). Obviously, the efficiency is power dependent which can be understood in terms of the proportionality of the elastic amplitude

Table I. Efficiencies of Various Materials

Material	η/I_o
fused quartz	1.2×10^{-12}
pyrex	1.2×10^{-14}
Mo	1.2×10^{-12}
water	2.1×10^{-12}
acetone	5.3×10^{-10}
liquid He(4.2°K)	7.6×10^{-11}
	$\sim 1 \times 10^{-5}$

Elastic conversion efficiency per unit (w/cm^2) absorbed optical flux for a clamped homogeneous medium based on Eq. (6).

on incident optical power density. Since the conversion efficiencies are low, especially for solids, it becomes important to determine what maximum power densities can be used without damage to the material under test or the intermediate thermoelastic generating structure. For this reason we have calculated a number of temperature-time profiles resulting from gaussian laser pulses incident on plates of aluminum and steel submerged in water.[4] Here the water acts to clamp or constrain the absorbing metal surface. From these heating and cooling curves (Fig. 1), it is found that maximum laser power densities on the order of $10^7 w/cm^2$ can be absorbed without damage (melting)

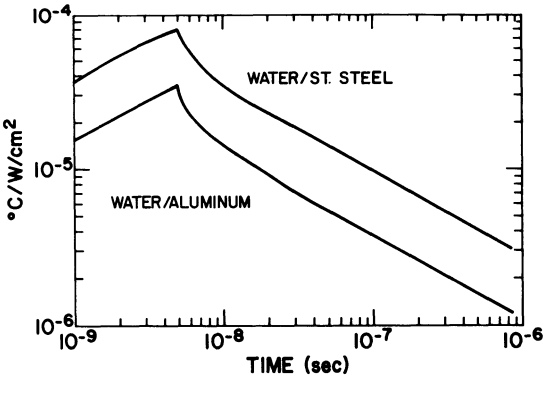

Fig. 1. Thermal profiles for 5 ns heating for $1 w/cm^2$ of absorbed power of steel and aluminum, each in water. The beam was assumed to be gaussian with half width, r_o = 50 μm.

to these two materials. When pulse repetition rates become greater than $\sim$10 pps, DC heating will occur, further diminishing the allowable absorbed power density. The conversion efficiency to a 10 MHz elastic wave from the 5 ns optical pulse is determined by the bandwidth of the detector (here $\sim\pm$2.5 MHz) and the effective optical power in that portion of the Fourier spectrum. We have estimated the latter to be $\sim$5% of the total power in the pulse with the assumptions that the net optical power resulting for $2 \times 10^7 w/cm^2$ absorbed by steel in the range 10±2.5 MHz will be only $9.5 \times 10^5 w/cm^2$. For a beam of $10^{-2} cm^2$ cross sectional area, Eq. (6) predicts (perfect clamping using a thermal insulator) only $\sim 10 w/cm^2$ conversion. For a beam area of $10^{-2} cm^2$ and an acoustic reflection coefficient between steel and water of 0.1, a net available power of only 10 mW results. A summary of some relevant parameters relating optical to elastic conversion efficiencies for aluminum and steel is given in Table II.

We have investigated several schemes to increase the available acoustic power without effecting substantially the conversion efficiency at the region of absorption. This basically requires the availability of large laser powers which can be distributed over large areas to avoid material damage and simultaneously some means for collecting or focusing the acoustic energy derived from the large area source. We have investigated two types of generating structures to achieve these goals: (1) thermoelastic holograms, and (2) thin film coated concave optical lenses.[5] The laser energy was distributed over areas up to $\sim 1.5 cm^2$. This is in contrast with earlier work at 20 MHz were the optically absorbing areas were $\sim 0.01 cm^2$-$0.04 cm^2$. A frequency doubled Q-switched Nd-YAG laser at 530 nm (pulse width $\sim$20 ns) was used at repetition rates of 5 and 10 pps with peak powers of $\sim$5 MW.

Table II. Parameters for Aluminum and Steel

Material	Max. absorbed flux (w/cm^2) (1)	Effective flux at 10 MHz (w/cm^2) (2)	Efficiency η (3)
Al	1.7×10^7	8.5×10^5	1.5×10^{-5}
Steel	1.9×10^7	9.5×10^5	1.1×10^{-5}

Parameters for Al and Steel (1) Maximum absorbed flux in 5 ns pulse to prevent melting with sample in water, based on Fig. 1; (2) Effective flux at 10±2.5 MHz based on Fourier analysis of input light pulse; (3) Efficiency based on Eq. (6) assuming perfect clamping and the absorbed power density of (2).

The principle of the thermoelastic holographic scheme is shown in Fig. 2. With the interference of a point source and a plane wave, the former distance ℓ from the hologram and 3 cm measured along the normal to the plane at an angle of $\sim 47°$. The propagation velocity is taken 1.5×10^5 cm/s, the speed of sound in water. The loci of constant phase $\Theta = 2\pi\ell/m\lambda$ are determined by the relation

$$x^2 + y^2 + z_o^2 = m^2\lambda^2 \quad . \tag{7}$$

Here λ is the acoustic wavelength at 10 MHz in water (1.5×10^{-2} cm) and m is an integer. The regions of constant phase define the hologram since plane acoustic waves illuminating a structure absorbing and transmitting according to this phase pattern will result in a plane wave at the zero order of interference and a wave that focuses at the location of the point source. Similarly, a thermoelastic structure, where the modulated phase fronts correspond to regions of optical absorption and reflection will also generate a plane and a focused acoustic wave, Fig. 3.

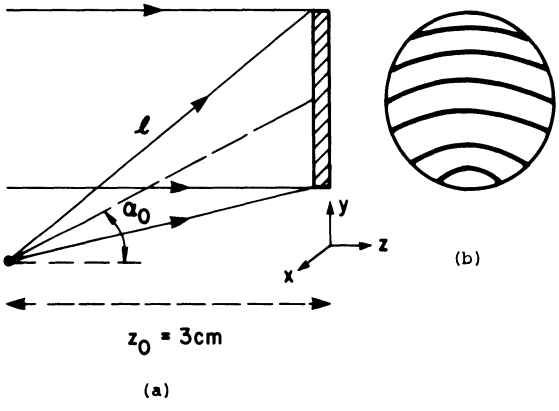

Fig. 2. Diagram for calculating the hologram. The hologram is shown in (b). Illumination of this hologram in water in conjunction with a rubber membrane will cause a thermoelastic wave to focus at the point located 3 cm from the hologram measured along the normal. 2b shows the hologram with regions of constant phase.

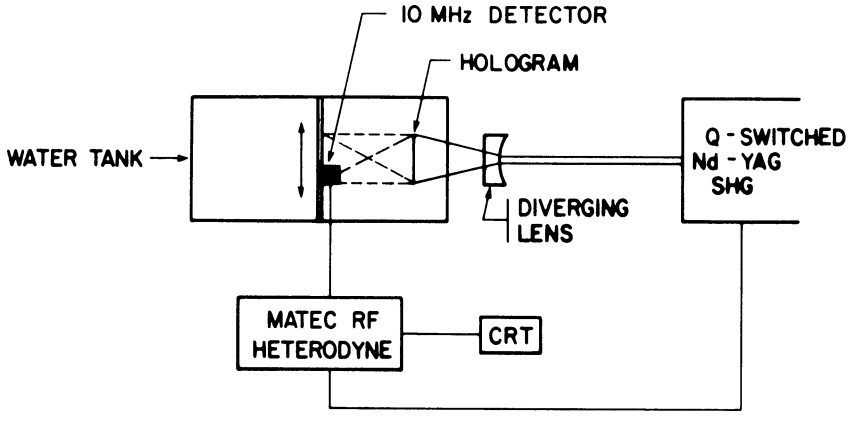

Fig. 3. Experimental water tank and associated equipment for holographic data.

The phase fronts for the holographic structure were calculated in closed form and from the resulting pattern a photolithographic mask was constructed. Holograms were made from these masks with patterns such as those shown in Fig. 2b deposited on glass. The darkened curved regions are silver evaporated films and are adjacent to regions where maximum phase is required. Black epoxy paint or a cemented rubber membrane was used to provide optical absorption and generate elastic waves in those regions. Thus, laser light was alternately absorbed by the paint and reflected by the silver.

Our experiments were made in a plexiglass water tank, transparent to the incident laser light (Fig. 3). A movable 10 MHz, 6 mm diameter PZT detector was connected to a tuned RF heterodyne receiver (Matec). Data of acoustic amplitude as a function of position was recorded as shown in Fig. 4. The relatively weak signal in the first order peak can be ascribed to (1) lack of a blaze angle, (2) lack of grey scale in the holographic pattern, (3) relatively wide bandwidth of receiver and RF circuit, and (4) the use of pulse excitation rather than 10 MHz sinusoidal optical modulation.

From the data (Fig. 4) it was determined that the first order peak occurred at an angle of $\sim 54°$ with respect to the normal of the hologram compared to the 47° design angle. No first order peak was observed on the opposite side of the zero order peak, consistent with that being a region of virtual focus. Although the intensity of the focused peak was quite small, these preliminary measurements should serve as a demonstration of feasibility for the potentially large energy densities that can be derived from thermoelastic holographic techniques.

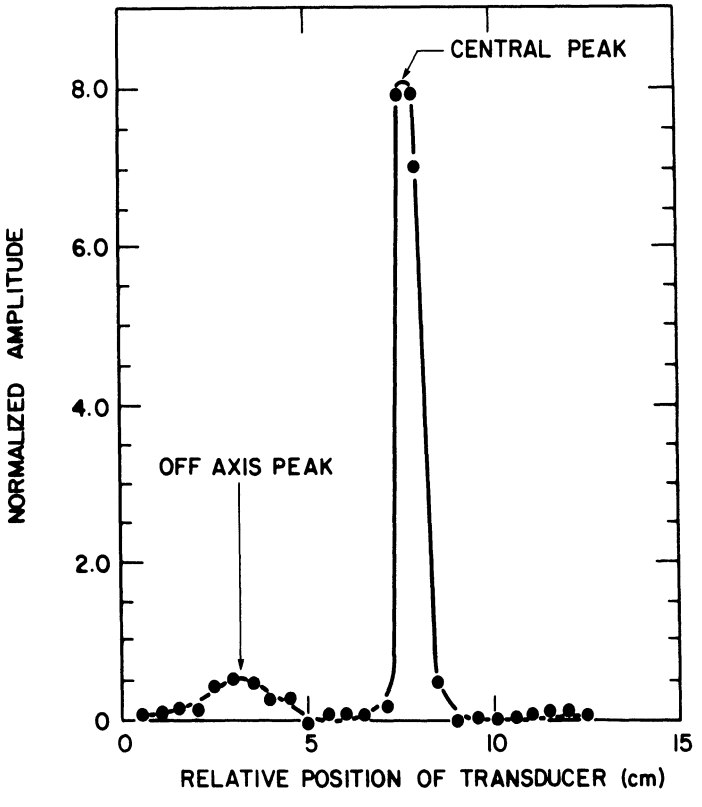

Fig. 4. Data showing off-axis first order acoustic amplitude peak.

The thermoelastic thin film-glass lens structure tested as an elastic wave generator had the following characteristics: a nickel thin film 2900 Å thick, evaporated onto the concave face of the lens, lens diameter 5 cm and radius of curvature equal to 9.1 cm. The extent of elastic wave focusing at 10 MHz was measured by recording the amplitude as a function of position, z, for several laser spot diameters. As shown in Fig. 5, a thin acoustically absorbing rubber diaphragm was placed over the 6 mm diameter detector to limit the effective aperture to 0.25 mm, thereby reducing the phase cancellation that occurs when spherical waves are incident on a flat phase sensitive receiver. Figure 6 shows a plot of amplitude as a function of position, with the peak occurring at $\sim$58μs. This time was measured on an oscilloscope and is the difference between the acoustic detector arrival time relative to t_o, the onset of the laser pulse. We attribute the somewhat earlier observed arrival time to that predicted as a result of misalignment of the detector with respect to

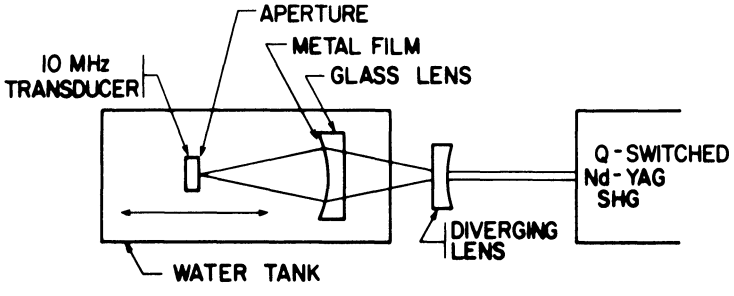

Fig. 5. Experimental arrangement for distributing laser energy over large area of an elastic generator resulting in a focusing propagating wave. Detection used with a 0.25 mm aperture placed over the 10 MHz PZT. Output of the PZT was connected to an RF heterodyne circuit similar to that of Fig. 4.

the axis of the lens (giving rise to a smaller path length for the acoustic wave).

Although we have not yet demonstrated the ability to obtain large acoustic powers from either of the structures described in this paper, we feel that feasibility has been well demonstrated. Additional holographic schemes with scanning capability are presently under consideration.

ACKNOWLEDGEMENT

We are grateful to Dr. R. Hodgson for the use of his Q-switched laser and helpful discussions concerning its operation in these experiments.

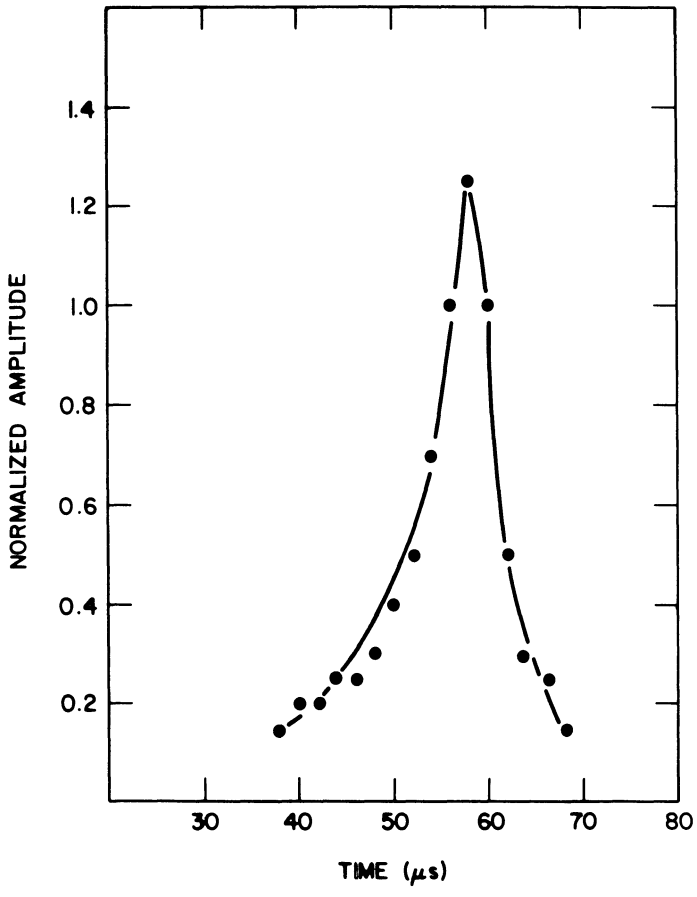

Fig. 6. Data from the arrangement of Fig. 5 showing the acoustic amplitude peak as a result of focusing the acoustic wave by the curved thermoelastic generating structure.

REFERENCES

1. R.M. White, JAP 34, 3559, 1963.
2. R.J. von Gutfeld and R.L. Melcher, APL 30, 257, 1977, R.J. von Gutfeld and R.L. Melcher, Materials Evaluation 35, 97, 1977.
3. R.J. von Gutfeld and H.F. Budd, APL 34, 617, 1979.
4. R.J. von Gutfeld, Report No. NADC-78240-60; R.J. von Gutfeld, Ultrasonics 18, 175, 1980.
5. R.W. Dreyfus, E.E. Tynan and R.J. von Gutfeld, U.S. Patent No. 4,269,067.